Digest Journal of Nanomaterials and Biostructures Vol. 13, No. 1, January - March 2018, p. 299 - 305

DESIGN OF HIGH-EFFICIENCY TANDEM DYE-SENSITIZED SOLAR CELL WITH TWO-PHOTOANODES TOWARD THE BROADER LIGHT HARVESTING

A. K. ALI [a], S. E. ELA[b], K. I. HASSOON[a], C. ELA[c], D. S. AHMED[a*]
[a]*Applied Sciences Departments, University of Technology, Baghdad, Iraq*
[c] *Ege University, Solar Energy Institute, Bornova, 35100 Izmir, Turkey*
[b]*General Directorate of State Airports Authority, 35100 Izrnir, Turkey*

Tandem sensitized solar cell (TDSSCs) with various dyes is a promising device with broader harvesting efficiency of the solar spectrum. In this work, two dye sensitized solar cells (DSSCs) of organic dyes and different absorption regions are stacked together in parallel connection to construct tandem dye-sensitized solar cells with broader and more integrated absorption band. Gold nanorods (GNRs) were utilized as a scattering layer in the back face of the back cell. The results showed that TDSSC exhibited much higher conversion efficiency compared to single DSSCs. Efficiencies up to 11 % can be achieved using TDSSC in parallel connection. Moreover, charge transfer resistance R_{ct} decreased from 95 Ω to 54 Ω retaining about 76 percent improvement.

(Received November 13, 2017; Accepted March 13, 2018)

Keywords: Dye-sensitized solar cell, tandem, high conversion efficiency, N719, DSSC.

1. Introduction

Dye-sensitized solar cells (DSSCs) have attracted remarkable attention in the last three decades because of their low fabrication cost [1-3], simple manufacturing processes [4, 5], environmentally friendly materials and unique features such as high transparency and various color scalability [4]. The basic principle of tandem cell is to use several individual DSSCs or photo-electrodes [6, 7]. Because different DSSCs have different absorption bands, TDSSCs can take full advantage of sun light resulting in higher open circuit voltage and short circuit current. Consequently, TDSSCs have been proposed for several applications. For example, Ahn et al. [8] fabricated TDSSC with sufficient efficiency to drive electrochromic devices. Other authors used two DSSCs connected in series to supply energy for hydrogen production by water cleavage [9]. Although other types of photovoltaic devices such as thin film and perovskite solar cells show higher efficiency [10-12] than the standard DSSCs. However, DSSCs reveal a high price-to-performance ratio which makes them good competitor to their contemporary solar cells. There are many attempts have been employed to enhance the conversion efficiency of DSSCs. These attempts used various approaches such as employing various designs and thicknesses of TiO_2 [13-15], utilizing light-scattering layer [16], or hybrid combination of two dyes [17] and panchromatic dye layers [18]. A good aspect of the theoretical work of DSSCs is presented by Helma et al. [19] and Villanueva et al. [20].

One interesting problem is that in order to increase the light-collection ability of DSSCs, it is recommended to enhance the absorption of the dye which depends on the dye-material itself or to use thicker layer of TiO_2 [21]. When a thicker layer is utilized, the cell will have higher series resistance. To solve this problem, a tandem structure of two single DSSCs is proposed [22]. In this respect, TiO_2 layers which are used as photo-electrodes in the DSSCs should have good transparency and conductivity.

*Corresponding author: duhasaasd2015@gmail.com

We think that the technique of using tandem-structured is one of the very good solutions to enhance the performance of DSSCs [6, 23]. In this work, we used two different dyes to construct tandem dye sensitized solar cell.

2. Experimental section

2.1. Fabrication of Tandem Dye Sensitized Solar Cells

FTO glass plates (TEC15, Dyesol) with sheet resistance 15 Ω/sq. are used as substrates for the working and counter electrodes. Several FTO plates with areas of 2 cm × 1.5 cm are rinsed with deionized water, cleaned in acetone using ultrasonic bath for 25 min. TiO_2 paste (18NR-T, Dyesol) which consists mainly of TiO_2 nanoparticles with particle size ~20 nm is utilized to fabricate the photoanode. Doctor-blade method is implemented to place the TiO_2 paste between two Scotch tapes. When the paste becomes dry, the two tapes are removed and the TiO_2 mold is fired at 500°C for 30 min. The result is a transparent mesoporous TiO_2-layer with thickness of 10-12μm controlled by the scotch tape. A layer of gold nanorods (Sigma-Aldrich), with 25/35 nm in size and about 150 μg/ml in concentration were deposited on the back of TiO_2 films as a scattering layer. The TiO_2-layer in the front of DSSC is immersed in a solution of N719 dye (Dyesol), and then the back cell is immersed in 0.25 mM of RK1 dye (Solaronix) for 1 day to give the layer sufficient time for the soaking-up process. The counter electrode is fabricated by drop casting method of platinum paste (PT1, Dyesol) onto FTO substrates (TEC15, Dyesol). When the platinum paste becomes dry, it is also fired at 450°C for 30 minutes. After the firing process, the platinum film typically possessed high transparency and good conductivity. After that, two holes are drilled on the counter electrode to facilitate electrolyte injection. Thermoplastic sealant (Dyesol) in the form of casket is used to assemble the two electrodes. The electrolyte (I^-/I^{3-} redox couple) is injected inside the DSSCs via one of the holes in counter electrode. Fig. 1(a) shows an image of a single dye sensitized solar cell (SDSSC). To fabricate a tandem cell, two analogous DSSSs (C1and C2) are electrically connected in parallel as shown in Fig. 1(b). In order to select the photo-active area, the front face of the DSSC structure is covered with a black paper and shined through a hole of area 0.16 cm^2. The single cells are connected in a way presented earlier in Fig. 1(b) where C1 is chosen to be in the front and C2 in the back and tandem DSSCs introduced as (C3) made from two cells (C1+C2).

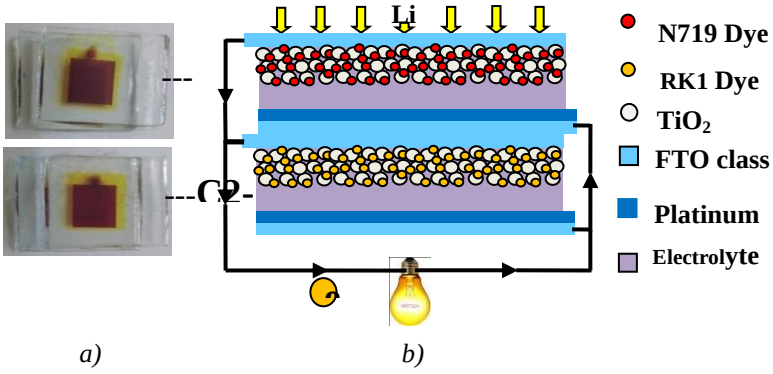

Fig. 1. (a) Top view images of N719 and RK1 DSSC were used in TDSSC, (b) cross-sectional view of TDSSC.

2.2. DSSCs Characterizations

The film thicknesses of photoanode were examined by profilometer (model Ambios Technology XP-1). Current-voltage (I-V) characteristics for single and tandem DSSCs are measured under illumination of AM1.5 condition (100 mW/cm^2) using Xenon lamp (type Oriel 450 W) as a source of light. Collection of I–V data is performed using LabView software. IPCE

equipment (type K3100 McScience) is employed to plot the external quantum efficiency as a function of wavelength. Finally, electrochemical measurements were carried out on a Zahner (IM6, Germany).

3. Results and Discussion

Fig. 2 shows absorption spectra of N719 and RK1 dyes in the spectral region from 350 nm to 700 nm. All the dyes show good absorbance in the visible region. Another interesting property is that RK1 shows high absorption in the region where N719 have limited absorbance.

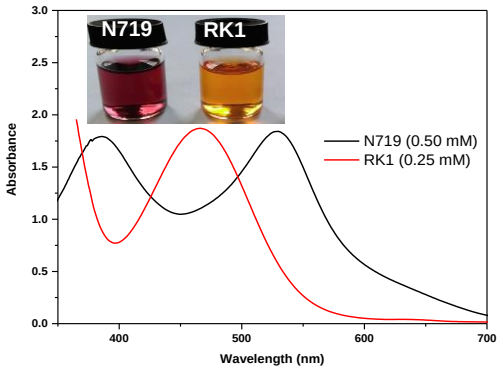

Fig. 2. Absorbance of N719 and RK1 dyes were used in TDSSC

As can be seen from Fig.3, the quantum efficiency of incident photon-to-collected electron IPCE-curves sustains their peaks in the spectral range 475-550 nm. The IPCE curve of N719 and RK1 DSSCs based on semitransparent TiO_2 reveals clear maximum around 550 and 450 nm, respectively.

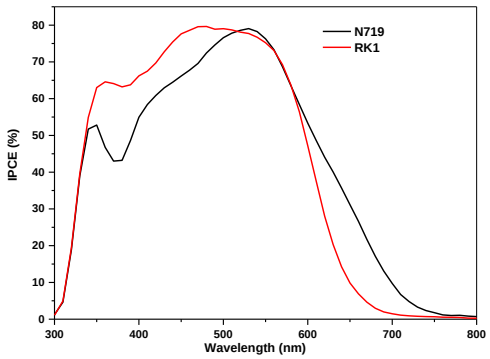

Fig .3. IPCE of individual of N719 and RK1 dyes, were used in TDSSC

Fig. 4 shows rectangle of maximum power for the single DSSCs with N719 and RK1 as the active dyes were introduced as (C1 and C2) and tandem DSSCs introduced as (C3) made from two different dyes. Tandem cell revealed higher current density and larger area under the J-V curve (higher filling factor) than those for single cells. With respect to parallel connection, the short circuit current density J_{sc} for C3 is almost equivalent to C1+C2, while the open circuit voltage V_{OC} equivalent to smallest one. The photovoltaic parameters of single and tandem cells are summarized in Table 1.

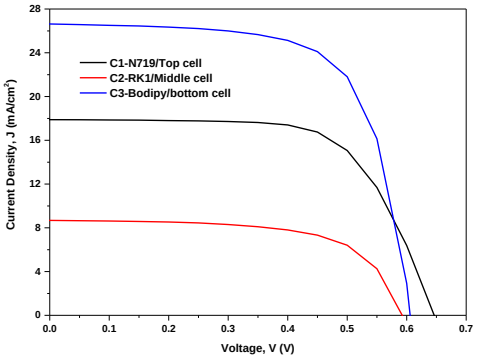

Fig.4. (I–V) characteristics for three cells, front cell (C1), and back cell (C2), were integrated in TDSSC (C3) in parallel connection.

Table 1. Solar cell parameters for single and Tandem DSSCs, η(%) is the mean of the solar conversion efficiency.

Cells	J_{sc} (mA/cm^2)	V_{oc}(V)	FF	η(%)
C1- N719/Front cell	17.90	0.65	0.66	7.68
C2- RK1/ back cell	8.68	0.60	0.64	3.33
C3- Tandem (C_1+C_2)	26.62	0.60	0.69	11.02

Table1 shows some of the calculated parameters namely: short circuit current density (J_{SC}), open circuit voltage (V_{OC}), conversion efficiency (η) and fill factor (FF). As can be seen from Table 1, the highest conversion efficiency is about 11 % for tandem parallel cell (C3) with J_{SC} = 26.62 mA/cm^2, V_{OC} = 0.6 V and FF= 0.69.

3.1. Electrochemical Impedance Spectroscopy

To examine the electron transfer and transport processes in DSSCs, electrochemical impedance spectroscopy (EIS) properties were studied for single and tandem DSSCs. Fig. 5 show the EIS spectra for dark condition under applied forward bias voltage of 0.65 V. The frequency range is between 100 mHz to 1 MHz. Nyquist plots of EIS spectra reveals two semicircle. The radius of the second one (the larger semicircle) in the medium frequency range (1-100 Hz) is related to the charge-transfer resistance R_{ct} at TiO_2/dye/electrolyte. The first semicircle (small circle) radius in the high frequency range (10^2-10^6) represents the charge-transfer resistance R_{ce} at the counter electrode/electrolyte interface. [24, 25]. The impedance in the low-frequency range depends on Warburg diffusion mode of I^-/I^{3-} in the electrolyte [26, 27]. An Ohmic resistance, starting point of the intersection of the frequency at the real resistance axis symbolizes in Fig. 5(a) corresponds to series resistance R_s. The R_s is mainly due to the FTO sheet resistance and contact between electrodes and the substrates. The performed Nyquist plots and Bode phase plots of C1, C2 and C3 are compared in Fig. 5(a) and Fig.5 (b), respectively. The EIS parameters are taken away from the recorded EIS results and summarized in (Table 2). The electron life time and electron recombination rate were estimated according to the following equations 1, and 2, respectively: [28]

$$\tau_e = 1/2\pi f \quad (1)$$

$$K_{eff} = 1/\tau_e \quad (2)$$

f is the peak frequency which corresponds to the second semicircle in the Nyquis plots, K_{eff} represents the electron recombination rate [28].

The results reveal that the electron transport resistance, R_{ct}, of tandem cell is 54 Ω, which is smaller than those of the individual C1and C2 are 95 and 112 Ω, respectively Table 2. The low

R_{ct} value, which is suitable for rapid charge transport [29], is attributed to the sum of resistors in parallel circuit connection of tandem cell.

The R_{ce}, can be evaluated from the first semicircle of Nyquist plots. The R_{ce} values 10, 21and 7 Ω are corresponding to C1, C2 and C3, respectively. The smaller R_{ce} value of tandem cell is attributed to parallel connection. According to maximum frequency f of the second semicircle Fig. 5; the electron life time τ_e were 42, 25 and 42 ms for C1, C2and C3, respectively. The enhanced value of τ_e for tandem cell may be due to decreased recombination rate. The high value τ_e is expected to be the origin of high J_{SC} and η of the fabricated cell. The recombination rate, K_{eff}, is 23.8, 31.2, 40 and 23.8 s^{-1}, and low K_{eff} in tandem cell is attributed to small resistance R_{ct} and R_{ce} promoted fast charge transfer and transport, As elucidated above, and leads to promoted FF, desirable for good efficiency solar cells. Previous EIS studies on DSSCs suggest that the photovoltaic results η and J_{SC}, being inversely proportional to R_{ct} as well as R_{ce} [30, 31] opposite to that of the overall efficiency (see Table 1 and Table 2). i.e. the lowest value of R_{ct} presents the largest value of efficiency and vice versa.

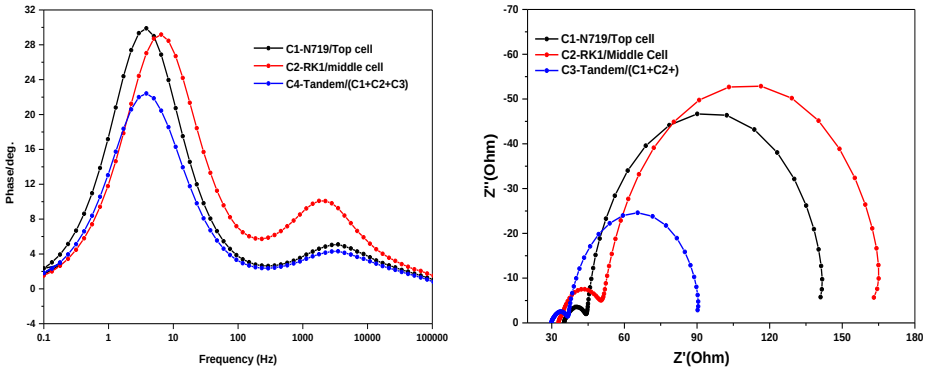

Fig. 5. EIS of the C1/N719 (Black line), C2/RK1 (Red line), and C3/Tandem (Blue line) in the forms of Nyquist phase plot (a) and Bode phase plot (b) respectively

Table 2. EIS results of the fitting parameters R_{ct}, R_{ce}, τ and K_{eff} included in Fig. 5.

Cells	R_{ct} (Ω)	R_{ce} (Ω)	R_s (Ω)	τ (ms)	K_{eff} (s^{-1})
C1- N719/front cell	95	10	35	42	23.8
C2- RK1/ back cell	112	21	33	25	40
C3- Tandem/(C_1+C_2)	54	7	30	42	23.8

4. Conclusions

We calculated photovoltaic parameters for parallel-connected tandem DSSCs and compared them with single DSSCs. Single DSSCs with dyes having different but complementary spectral absorption bands can be connected in parallel to fabricate tandem solar with improved properties. Compared with single DSSCs, tandem DSSCs show higher conversion efficiency, greater fill factor and lower R_s and R_{ct}. IPCE-spectrum suggests using complimentary dye as RK1 with N719 to increase the absorbed spectrum in the visible and infrared regions. Our results showed that DSSCs with tandem design has the ability to improve the photovoltaic parameters. EIS results can be used to study the electron transport and charge recombination processes in tandem DSSCs.

Acknowledgements

This work is supported by Ege University/ Solar Energy Institute Bornova, 35100 Izmir, Turkey and Department of Applied Sciences, University of Technology, Baghdad, Iraq.

References

[1] W. Kubo, Ayumi Sakamoto, Takayuki Kitamura, Yuji Wada, Shozo Yanagida, Journal of Photochemistry and Photobiology A: Chemistry **164**, 33 (2004).
[2] A. C. Cakir, Sule Erten-Ela, Advanced Powder Technology **23**, 655 (2012).
[3] X.-Z. Guo, Yi-Duo Zhang, Da Qin, Yan-Hong Luo, Dong-Mei Li, Yu-Tong Pang, Qing-Bo Meng, Journal of Power Sources **195**, 7684 (2010).
[4] H. Seo, Shinji Hashimoto, Daiki Ichida, Naho Itagaki, Kazunori Koga, Masaharu Shiratani, Electrochimica Acta **179**, 206 (2015).
[5] Mohammed A. Al-Azawi, Noriah Bidin, Abdulrahman K. Ali, M. Bououdina J Mater Sci: Mater Electron **26**, 6276 (2015).
[6] C.-F. Chi, Song-Chuan Su, I-Ping Liu, Cheng-Wen Lai, Yuh-Lang Lee, J. Phys. Chem. C **118**, 17446 (2014).
[7] M. Murayama, T. Mori, J. Phys. D: Appl. Phys. **40**, 1664 (2007).
[8] K.-S. Ahn, Sung Jong Yoo, Moon-Sung Kang, Ji-Won Lee, Yung-Eun Sung, J. Power Sources **168**, 533 (2007).
[9] L. Andrade, Rui Cruz, Helena Aguilar Ribeiro, Adélio Mendes, Int. J. Hydrogen Energy **35**, 8876 (2010).
[10] A. Kojima, K. Teshima, Y. Shirai, T. Miyasaka, Organometal Halide Perovskites as Visible-Light Sensitizers for Photovoltaic Cells, J. Am. Chem. Soc. **131**, 6050 (2009).
[11] M. M. Lee, J. Teuscher, T. Miyasaka, T. N. Murakami, H. J. Snaith, Science **338**, 643 (2012).
[12] J. Burschka, N. Pellet, S. Moon, R. Humphry-Baker, P. Gao, M.K. Nazeeruddin, Michael Grätzel, Nature **499**, 316 (2013).
[13] W. Zhao, Hari Bala, Jingkuo Chen, Yujie Zhao, Guang Sun, Jianliang Cao, Zhanying Zhang , Electrochimica Acta **114**, 318 (2013).
[14] M. C. Kao, H. Z. Chen, S. L. Young, C. Y. Kung, C. C. Lin, Thin Solid Films **517**, 5096 (2009).
[15] X. Zhang , Bailiang Xue, Wenming Liao, Wei Liu, Wei Mu, Zh iqun Lin Dajia ng Zheng, Yulin Deng Yusheng, J. Mater . Chem. A, **2**, 11035 (2014).
[16] L. Zhu, Y. L. Zhao, X. P. Lin, X. Q. Gu, Y. H. Qiang. Superlattices and Microstructures **65**, 152 (2014).
[17] S. K. Balasing, Minoh Lee, Man Gu Kang, Yongseok Jun, Chem. Commun. **49**, 1471 (2013).
[18] R. Y. Ogura, Shigeru Nakane, Masahiro Morooka, Masaki Orihashi, Yusuke Suzuki, Kazuhiro Noda, Appl. Phys. Lett. **94**, 073308 (2009).
[19] J. Halme, Paula Vahermaa, Kati Miettunen, Peter Lund, Adv. Mater. **22**, E210 (2010).
[20] J. Villanueva, Juan A. Anta, Elena Guillé, and Gerko Oskam, J. Phys. Chem. C **113**, 19722 (2009).
[21] H. Zhang, W. Wang, H. Liu, R. Wang, Y. Chen, Z. Wang Materials Research Bulletin **49**, 126 (2014).
[22] M. Durr, A. Bamedi, A. Yasuda, G. Nelles Appl. Phys. Lett. **84**, 3397 (2004).
[23] S.-Q. Fan, Baizeng Fang, Hyunbong Choi, Sanghyun Paik, Chulwoo Kim, Ban-Seok Jeong, Jeum-Jong Kim, Jaejung Ko, Electrochimica Acta **55**, 4642 (2010).
[24] F. Fabregat-Santiago, J. Bisquert, E. Palomares, L. Otero, D. Kuang, S.M. Zakeeruddin, M. Gratzel, J. Phys. Chem. *C* **111**, 6550 (2007).
[25] J. v. d. Lagemaat, N.-G. Park, A. J. Frank J. Phys. Chem. B **104,** 2044 (2000).
[26] Q. Wang, J.-E. Moser, M. Grätzel, J. Phys. Chem. B **109**, 14945 (2005).
[27] A. Shit, S. Chatterjee and A. K. Nandi, Phys. Chem. Chem. Phys. **16**, 20079 (2014).
[28] M. Adachi, Masaru Sakamoto, Jinting Jiu, Yukio Ogata, Seiji Isoda, J. Phys. Chem. B **110**(28), 13872 (2006).

[29] N. Fu, Chun Huang, Yan Liu, Xing Li, Wei Lu, Limin Zhou, Feng Peng, Yanchun Liu, Haitao Huang, ACS Appl. Mater. Interfaces **7**, 19431 (2015).
[30] A. L. Viet, R. Jose, M. V. Reddy, B. V. R. Chowdari, S. Ramakrishna, J. Phys. Chem. C, **114**, 21795 (2010).
[31] O. O. Ogunsolu, Jamie C. Wang, Kenneth Hanson, ACS Appl. Mater. Interfaces **7**, 27730 (2015).